

Suppression in the negative bias illumination instability of Zn-Sn-O transistor using oxygen plasma treatment

Cite as: Appl. Phys. Lett. **99**, 102103 (2011); <https://doi.org/10.1063/1.3634053>

Submitted: 15 July 2011 . Accepted: 18 August 2011 . Published Online: 07 September 2011

Shinhyuk Yang, Kwang Hwan Ji, Un Ki Kim, Cheol Seong Hwang, Sang-Hee Ko Park, Chi-Sun Hwang, Jin Jang, and Jae Kyeong Jeong



View Online



Export Citation

ARTICLES YOU MAY BE INTERESTED IN

[Effect of high-pressure oxygen annealing on negative bias illumination stress-induced instability of InGaZnO thin film transistors](#)

Applied Physics Letters **98**, 103509 (2011); <https://doi.org/10.1063/1.3564882>

[O-vacancy as the origin of negative bias illumination stress instability in amorphous In-Ga-Zn-O thin film transistors](#)

Applied Physics Letters **97**, 022108 (2010); <https://doi.org/10.1063/1.3464964>

[Photon-accelerated negative bias instability involving subgap states creation in amorphous In-Ga-Zn-O thin film transistor](#)

Applied Physics Letters **97**, 183502 (2010); <https://doi.org/10.1063/1.3510471>

Lock-in Amplifiers

... and more, from DC to 600 MHz



Suppression in the negative bias illumination instability of Zn-Sn-O transistor using oxygen plasma treatment

Shinhyuk Yang,^{1,2} Kwang Hwan Ji,³ Un Ki Kim,⁴ Cheol Seong Hwang,⁴ Sang-Hee Ko Park,¹ Chi-Sun Hwang,¹ Jin Jang,² and Jae Kyeong Jeong^{3,a)}

¹*Oxide Electronics Research Team, Electronics and Telecommunications Research Institute, Daejeon 305-700, Korea*

²*Department of Information Display, Kyung Hee University, Seoul 130-701, Korea*

³*Department of Materials Science and Engineering, Inha University, Incheon 402-751, Korea*

⁴*Department of Materials Science and Engineering, WCU Hybrid Materials Program, and Inter-university Semiconductor Research Center, Seoul National University, Seoul 151-742, Korea*

(Received 15 July 2011; accepted 18 August 2011; published online 7 September 2011)

This study examined the effect of oxygen plasma treatment on light-enhanced bias instability in Zn-Sn-O (ZTO) thin film transistors (TFTs). The treated ZTO TFT exhibited only a threshold voltage (V_{th}) shift of -2.05 V under negative bias illumination stress (NBIS) conditions, whereas the pristine device suffered from a negative V_{th} shift of 3.76 V under identical conditions. X-ray photoelectron spectroscopic analysis revealed that the oxygen vacancy defect density was diminished via the oxygen plasma treatment. This suggests the V_{th} degradation under NBIS is due to photo-transition of oxygen vacancy defects. © 2011 American Institute of Physics. [doi:10.1063/1.3634053]

Multi-component metal oxide thin film transistors (TFTs) have been intensively studied for their perspective applications in novel active-matrix (AM) display, such as a transparent and/or bendable AM display, because they offer the advantages of high field-effect mobility, optical clarity, excellent electrical uniformity, and low processing temperature.¹⁻³ In particular, the ZnO-based semiconductor has a wide band-gap (>3.0 eV) that enables the transparent electronics or display to be realized. The intriguing transparent aspect, however, should be carefully exploited, because sunlight or ambient light through the transparent electronic devices can cause a significantly reliability concern in conjunction with the electrical bias and/or thermal stress. The application of the negative bias illumination stress (NBIS) in metal oxide TFTs causes the serious threshold voltage (V_{th}) shift in the negative voltage direction, while the positive bias illumination stress (PBIS)-induced instability is relatively negligible.⁴ This extreme asymmetric deterioration can be understood by considering the trapping or injection mechanism of the photo-created hole carriers.⁵ The validity of the hole trapping model has been confirmed by the strong gate dielectric material dependence on the NBIS instability of the resulting oxide TFTs.^{6,7} Recently, an entirely different degradation mechanism has been proposed, based on the photon-transition model from the neutral oxygen vacancy [V_O] to double positive charged oxygen vacancy [V_O^{2+}].^{8,9} Ji *et al.* reported that the removal of the [V_O] defect center, via intentional oxygen diffusion, results in the strong suppression of NBIS instability in the InGaZnO TFTs. This supports the involvement of the oxygen vacancy defect.¹⁰ Thus, the origin of NBIS instability in oxide TFTs is still under debate. In addition, from the viewpoint of the actual application of the metal oxide TFTs, it is urgent to develop a practi-

cal process to prevent NBIS instability, as well as its complete clarification.

In this letter, we report the effect of oxygen plasma treatment on the NBIS-induced instability of Zn-Sn-O (ZTO) TFTs. We chose the ZTO semiconductor as a channel layer of the metal oxide TFTs, because the most popular InGaZnO system components are rare in the earth crust, as well as the expensive cost of In and Ga cations. Compared to the pristine device, the treated ZTO TFTs exhibited more stable behavior against the application of NBIS. This result can be explained by the V_O transition model. This was confirmed by x-ray photoelectron spectroscopy (XPS) data.

The fabricated ZTO TFTs have a bottom gate (BG) and bottom contact configuration. Lithographically patterned indium tin oxide (ITO) 150 nm thick on a glass substrate, with an area of 100×100 mm², was used as the gate electrode for the BG TFT. A 176 nm thick Al₂O₃ film as a gate insulator was deposited by atomic layer deposition (ALD) at a temperature of 150 °C. ZTO films with thicknesses of 20, 40, and 60 nm as a channel layer were grown using metal organic chemical vapor deposition (MOCVD). The fundamental details regarding the MOCVD-derived channel layer will be published elsewhere. Oxygen plasma treatment was performed on the ZTO/ITO/Al₂O₃/ITO/glass substrate. The plasma power and treated time were 500 W and 60 s, respectively. ALD-derived 9-nm-thick Al₂O₃ films were deposited as a passivation (or protective) layer on a ZTO/Al₂O₃/ITO/glass substrate, which was followed by the patterning of the active layer/Al₂O₃ stack simultaneously. The thermal contact annealing was performed at 250 °C for 2 h. The electrical measurements were performed at room temperature in air using an Agilent B1500A precision semiconductor parameter analyzer.

Figure 1 shows the transfer characteristics of the pristine ZTO TFTs (reference device) and oxygen plasma-treated ZTO TFTs with $W/L = 40$ μm/20 μm, respectively. The extraction procedures for device parameters were described

^{a)} Author to whom correspondence should be addressed. Electronic mail: jkjeong@inha.ac.kr.

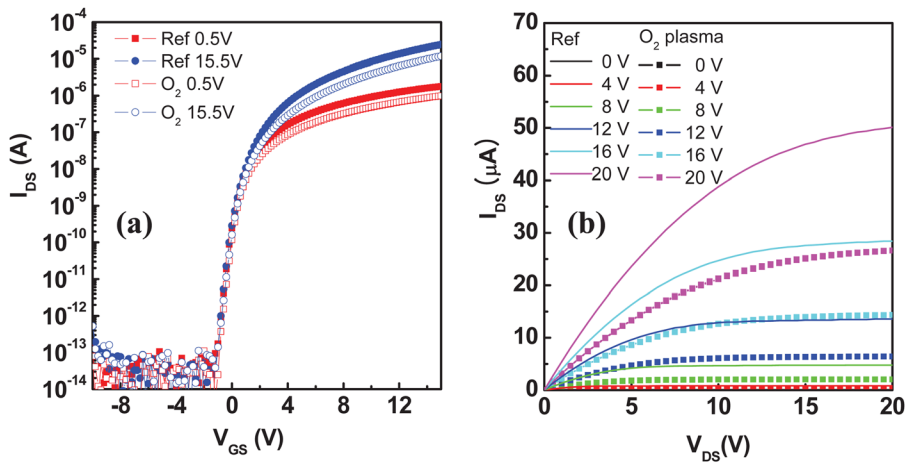


FIG. 1. (Color online) Representative (a) transfer and (b) output characteristics for both devices. Transfer curves were measured at $V_{DS}=0.5$ V and 15.5 V. Output curves were measured with increasing V_{GS} from 0 to 20 V (step size = 4 V).

in the previous report.¹⁰ It can be seen that the field-effect mobility (μ_{FE}) for the O_2 -treated device was slightly reduced from 4.97 cm^2/Vs (reference device) to 2.75 cm^2/Vs , which was reflected as the diminished drain current in the output characteristics, as shown in Fig. 1(b). In contrast, the sub-threshold gate swing (SS) for the O_2 -treated device improved from 0.43 V/decade (reference device) to 0.36 V/decade, suggesting that some of the tailing trap states can be cured by oxygen plasma treatment. The threshold voltage (V_{th}) and $I_{on/off}$ ratio for both devices were comparable to 1.3 – 1.5 V and 1 – 2×10^8 , respectively.

Figures 2(a) and 2(b) depict the evolution of transfer characteristics, as a function of NBIS duration for both devices. The devices were stressed under the following conditions: V_{GS} and V_{DS} were set to -20 V and 0 V at room temperature, respectively. The stress duration was $10\,000$ s. The full-width-at-half-maximum of the exposure to green light was approximately ± 10 nm near 530 nm and photo intensity was ~ 1 mW/cm^2 , as calibrated by photometry. It can be seen that the parallel V_{th} shift to the negative gate voltage with increasing NBIS time was observed for both devices without any significant change in the μ_{FE} , SS, and $I_{on/off}$ ratio. However, the amount of V_{th} movement for the ZTO TFTs during the application of NBIS strongly depends

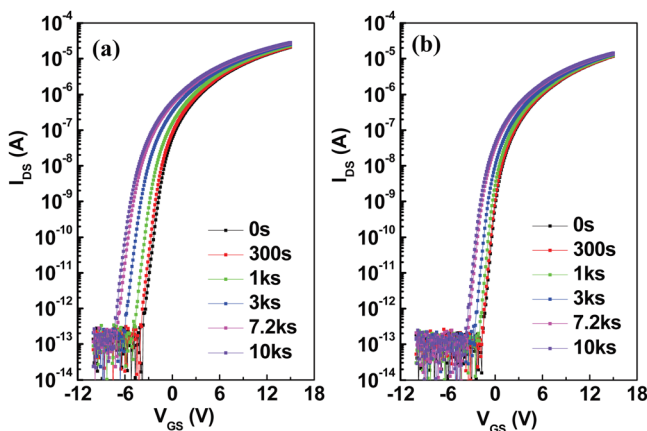


FIG. 2. (Color online) Evolution of the transfer curves for the (a) reference device and (b) the O_2 treated device with increasing NBIS time from 0 to $10\,000$ s at room temperature. Transfer curves during the NBIS duration were measured at $V_{DS} = 10$ V.

on the O_2 plasma treatment. The V_{th} value for the reference device was shifted approximately -3.76 V after NBIS for $10\,000$ s. In contrast, the negative V_{th} shift in the O_2 treated device was suppressed to ~ 2.05 V, as shown in Fig. 2(b).

The negative V_{th} shift in oxide TFT under NBIS has been attributed to the following three mechanisms, including the oxygen photo-desorption model,¹¹ the hole trapping model,^{5–7} and the photo-transition model from $[V_O]$ to $[V_O^{2+}]$.^{8–10} The first model can be explained by dynamic desorption of oxygen molecule/ions residing on the channel back surface by photon irradiation and subsequent donation of free electrons in the conduction band. In this study, the Al_2O_3 film, as a high quality passivation layer, was formed on the ZTO channel using atomic layer deposition. Therefore, we can exclude the possibility of the dynamical ambient interaction on NBIS instability. In addition, the photo-created hole trapping at or into the gate insulator cannot account for these observations, because the oxygen plasma treatment is unlikely to affect the underlying gate insulator interface and bulk region due to the protection of the ZTO channel layer. Thus, it would be quite reasonable to postulate that the oxygen vacancy model is responsible for NBIS instability. In a previous report, it was shown that the oxygen vacancy plays a crucial role in determining the V_{th} instability under NBIS condition.¹⁰ The deep state $[V_O]$ can be excited to the positively double charged $[V_O^{2+}]$ by light irradiation that gives the two delocalized free electron in the conduction band. This kind of behavior is well-known as the negative-U defect.¹² The lowering of the Fermi level near the oxide channel by the negative gate voltage during the NBIS duration would reduce the formation energy of $[V_O^{2+}]$, leading to the asymmetric V_{th} instability aforementioned.¹³ Thus, it can be understood that the oxygen plasma treatment decreases the concentration of $[V_O]$ via the in-diffusion of radical oxygen species into the back surface region of the ZTO channel. This speculation can be confirmed by the spectroscopic analysis of the oxygen chemical state in the ZTO thin film. Figure 3 shows their O 1s XPS spectra. The O 1s peaks centered at binding energies of 530.1 eV, 531.6 eV, and 533.5 eV are, respectively, related to oxygen in oxide lattices without oxygen vacancies, with oxygen vacancies, and with OH^- impurities.¹⁴ It can be clearly seen that the relative area of the oxygen vacancy-related peak

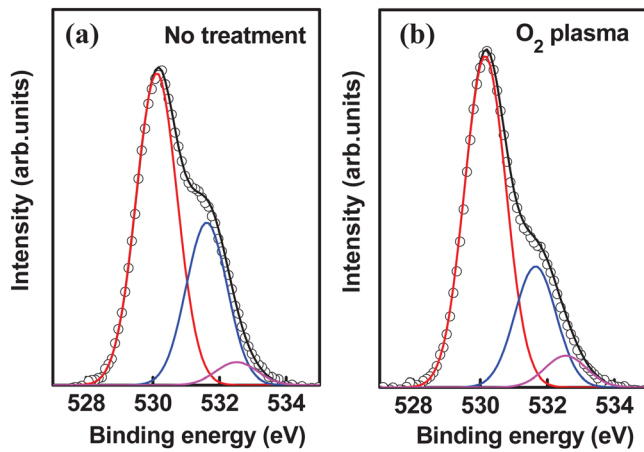


FIG. 3. (Color online) XPS O 1s spectra for the (a) reference ZTO and (b) O₂ treated ZTO thin films.

decreased by O₂ plasma treatment. The values are 33.3% and 25.0% for the reference and treated device, respectively. The strong correlation between [V_O] concentration and NBIS instability indicates that the improvement of photo-stability of the O₂ treated device arose from the reduction in [V_O] defect density. The creation of [V_O²⁺] by the photo-transition would be strongly dependent on the thickness of the channel layer, because the number of preexisting [V_O] defects will be proportional to the light-illuminated channel volume. Figure 4 shows the effect of channel thickness on NBIS induced V_{th} instability. It can be seen that the V_{th} shift

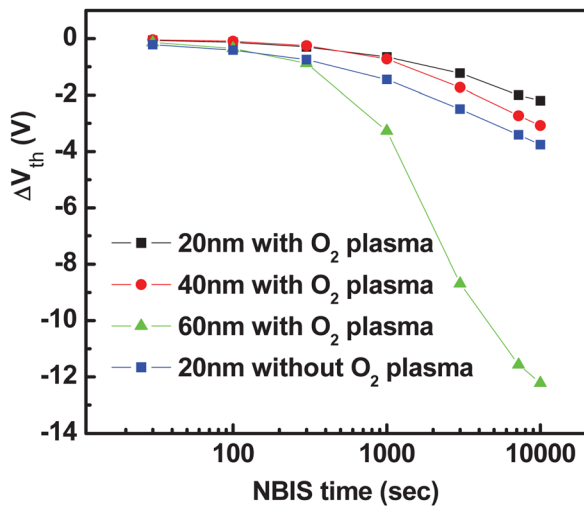


FIG. 4. (Color online) Variation in V_{th} value as a function of the applied NBIS time for the O₂ treated ZTO TFTs with different channel thickness (20 nm, 40 nm, and 60 nm). V_{th} variation for the reference device with 20 nm-thick channel is inserted for comparison.

for the 60 nm thick treated device was increased from -2.05 V (20 nm thick treated device) to -12.22 V. Therefore, the [V_O] based model is well corroborated with the fact that the V_{th} shift increased with increasing channel thickness of the ZTO thin film.

In summary, the V_{th} stability of the ZTO TFTs under NBIS conditions can be improved considerably by modest oxygen plasma treatment. The enhancement of photo-stability was attributed to the reduction in the concentration of [V_O] defect due to radical oxygen diffusion into the channel layer. This result supports the validity of the photo-transition mechanism from preexisting [V_O] to [V_O²⁺] for the plausible origin of the NBIS instability. Given that the oxide channel layer is not thick, the process of O₂ plasma treatment can be effectively implemented into the low temperature flexible electronics, as well as the transparent AM flat panel display, to secure the photo-bias stability of metal oxide TFTs due to its relatively low temperature processing.

This study was supported by the IT R&D Program of ETRI [Development of core technology for transmittance variable transparent display], the Nuclear Research and Development Program of NRF grant funded by the Korean government (MEST) (Grant code 2011-0002270), and the Inha University Research Grant.

¹K. Nomura, H. Ohta, A. Takagi, T. Kamiya, and H. Hosono, *Nature (London)* **432**, 488 (2004).

²M. K. Ryu, S. Yang, S.-H. K. Park, C.-S. Hwang, and J. K. Jeong, *Appl. Phys. Lett.* **95**, 173508 (2009).

³J. K. Jeong, J. H. Jeong, H. W. Yang, T. K. Ahn, M. Kim, K. S. Kim, B. S. Gu, H.-J. Chung, J.-S. Park, Y.-G. Mo, H. D. Kim, and H. K. Chung, *J. Soc. Inf. Disp.* **17**, 95 (2009).

⁴J.-H. Shin, J.-S. Lee, C.-S. Hwang, S.-H. K. Park, W.-S. Cheong, M. Ryu, C.-W. Byun, J.-I. Lee, and H. Y. Chu, *ETRI J.* **31**, 62 (2009).

⁵K.-H. Lee, J. S. Jung, K. S. Son, J. S. Park, T. S. Kim, R. Choi, J. K. Jeong, J.-Y. Kwon, B. Koo, and S. Lee, *Appl. Phys. Lett.* **95**, 232106 (2009).

⁶J.-Y. Kwon, J. S. Jung, K. S. Son, K.-H. Lee, J. S. Park, T. S. Kim, J.-S. Park, R. Choi, J. K. Jeong, B. Koo, and S. Y. Lee, *Appl. Phys. Lett.* **97**, 183503 (2010).

⁷K. H. Ji, J.-I. Kim, Y.-G. Mo, J. H. Jeong, S. Yang, C.-S. Hwang, S.-H. K. Park, M.-K. Ryu, S.-Y. Lee, and J. K. Jeong, *IEEE Electron Device Lett.* **31**, 1404 (2010).

⁸H. Oh, S.-M. Yoon, M. K. Ryu, C.-S. Hwang, S. Yang, and S.-H. K. Park, *Appl. Phys. Lett.* **97**, 183502 (2010).

⁹M. D. H. Chowdhury, P. Migliorato, and J. Jang, *Appl. Phys. Lett.* **97**, 173506 (2010).

¹⁰K. H. Ji, J.-I. Kim, H. Y. Jung, S. Y. Park, R. Choi, U. K. Kim, C. S. Hwang, D. Lee, H. Hwang, and J. K. Jeong, *Appl. Phys. Lett.* **98**, 103509 (2011).

¹¹S. Yang, D.-H. Cho, M. K. Ryu, S.-H. K. Park, C.-S. Hwang, J. Jang, and J. K. Jeong, *Appl. Phys. Lett.* **96**, 213511 (2010).

¹²B. Ryu, H.-K. Noh, E.-A. Choi, and K. J. Chang, *Appl. Phys. Lett.* **97**, 022108 (2010).

¹³A. Janotti and C. G. Van de Walle, *Appl. Phys. Lett.* **87**, 122102 (2005).

¹⁴K. W. Lee, K. M. Kim, K. Y. Heo, S. K. Park, S. K. Lee, and H. J. Kim, *Curr. Appl. Phys.* **11**, 280 (2010).